

# Sea Ice Research: Recent Findings and Outstanding Issues in Relation to Arctic Development

*Ed Ross and David B. Fissel*  
ASL Environmental Sciences Inc.  
Victoria, British Columbia, Canada

## ABSTRACT

Sea-ice research has made great progress over the past thirty to forty years due in large part to improved measurements arising from earth observing satellites and year-long continuous measurements of the underside of sea ice from below using subsurface instrumented moorings. The geometry of sea-ice is highly variable and complex with horizontal scale sizes of discrete sea-ice floes ranging from one meter or less to 50 km or more. The vertical scale size, or ice thickness, which is much harder to measure, ranges from 5 cm or less to over 50 m. Sea-ice motion is highly dynamic within the Arctic as indicated by large spatial variations over distance scales ranging from tens of meters to several thousand kilometers (basin scale) as well as on seasonal and interannual time scales. Large internal ice stress conditions can develop which result in the cessation of sea-ice motion which can also impede ship movements through the sea-ice. Given the highly deformed and fractured nature of the floating sea-ice cover, very different responses to nearly identical wind forcing of sea-ice floes can occur over distances as small as a few kilometers. The improved understandings of the sea-ice regime as realized from past, present, and future Arctic research, is essential to realizing the goal of safe and sustainable Arctic activities.

**KEY WORDS:** Sea-ice; velocity; thermodynamics; deformation; research; oceanography; Arctic.

## INTRODUCTION

The purpose of this paper is to provide a review and update of sea-ice research including recent findings. The paper also summarizes the outstanding sea-ice research issues which are important to Arctic development activities.

The motivation for sea-ice research has always involved geographic and scientific exploration of the vast and largely unknown Arctic, combined with national security and sovereignty dating back to the middle of the last century. In the latter part of the 20<sup>th</sup> century, sea-ice research broadened to address the needs of offshore oil and gas exploration and production (Hamilton, 2011). As the sea-ice extent in the Arctic has been reduced over the past two decades, the shipping

season for passages through the Arctic has been expanded along its continental margins through the Northern Sea Route off Russia and the Northwest Passage off Canada and the United States. Commercial shipping by ice-class vessels is already becoming more common, especially via the Northern Sea Route off Russia, and the prospect of shipping directly across the central Arctic Ocean is also being contemplated within the next few decades (Smith and Stephenson, 2013). To support Arctic shipping, sea-ice research is required for the development of safe and efficient shipping using these sea routes. In addition, sea-ice research is being conducted to study and better support the use of the Arctic by indigenous peoples who have traditionally used sea-ice as a means of transportation for subsistence hunting and travel based on the extensive traditional knowledge of sea-ice.

Conducting sea-ice research must overcome formidable challenges. These include: the remoteness and resulting high costs for conducting field studies and data collection in the Arctic; and the rapidly changing Arctic sea-ice regime which has become very apparent over the past 30-40 years (Meier et al., 2014). In addition, the complexity of the physical processes of sea-ice are very important.

## ARCTIC SEA-ICE FORMATION, PHYSICAL PROPERTIES AND REGIONAL DISTRIBUTION

The ice-covered seas which surround the poles of our planet represent about seven percent of the total area of the planet (Wadhams, 2000). Of this, the Arctic Ocean has sea-ice coverage of 15 million km<sup>2</sup> in winter which is reduced to 7 million km<sup>2</sup> in summer. In the Antarctic, by comparison, the area of sea-ice coverage is slightly larger at 18 million km<sup>2</sup> in winter, but this area is much more reduced in summer, amounting to only 3 million km<sup>2</sup> (NSIDC, 2018).

### Formation and Physical Properties of Sea-Ice

Sea-ice is simply frozen sea water which forms in the fall and winter months under the extremely low air temperatures in the Earth's polar regions. Initial formation of sea-ice occurs at the surface in the form of small platelets and needles called frazil ice crystals (Gow and Tucker, 1991). Under sheltered conditions, the frazil ice crystals freeze together to form a solid material with an initial thickness of 1 to 10 cm while under rough conditions with high turbulence levels, sea-ice forms as

frazil crystals which accumulate into slushy circular disks, called pancakes or pancake ice (NSIDC, 2018). The resulting solid sea-ice in the form of sheet ice has the structure of ice crystals which, as the ice develops, become increasingly oriented vertically, in alignment with the direction of heat losses as the ice continues to grow and develop. Sea-ice is a complex material that is composed of solid ice, dissolved salt in the form of brine, as well as gas and various types of solid salts (Timco and Weeks, 2010). Sea-ice is a unique physical feature, which is much different than freshwater or glacial ice. It behaves as a combination of a fluid and a solid material, the physics of which are quite different (Weiss, 2017; Feltham et al., 2006) than for other parts of the hydrosphere, including the atmosphere, ocean, and freshwater cryosphere. In dynamical terms, sea-ice behaves like a brittle elastic material in response to large- and small-scale deformation processes, although its rheology is complex (Girard et al., 2011; Dansereau et al., 2016).

As sea-ice forms, it progresses through observed stages of development which can be used by observers. Sea-ice charts make use of a classification system for characterizing sea-ice according to its observed stages of development, its ice concentration and nominal sizes of discrete ice floes according to WMO nomenclature, which is dubbed the “ice egg code” (Fig. 1). As formation proceeds, the thickness of sea-ice increases as given by the nominal range values of Fig. 1 which are applicable to undeformed sea-ice (sea-ice deformation processes are described below).

For the engineering properties of sea-ice, ice thickness is very important in determining the ice loads exerted by sea-ice on offshore structures and on marine navigation. As sea-ice progresses through its stages of development, its strength increases as the ice salinity and porosity of sea-ice decreases. First-year sea-ice (Fig. 1) has typical salinity ranges of 5.0 to 7.6 parts per thousand (Timco and Weeks, 2010). Old ice (second-year ice which has survived one summer or multi-year ice which has survived two or more summers) undergoes important structural changes with the summer warming resulting in the release of formerly solid salts into a liquid phase on warming, which then exit the sea-ice. The salinity of old ice can reach values as low as 1.5 to 2.0 parts per thousand (Timco and Weeks, 2010).

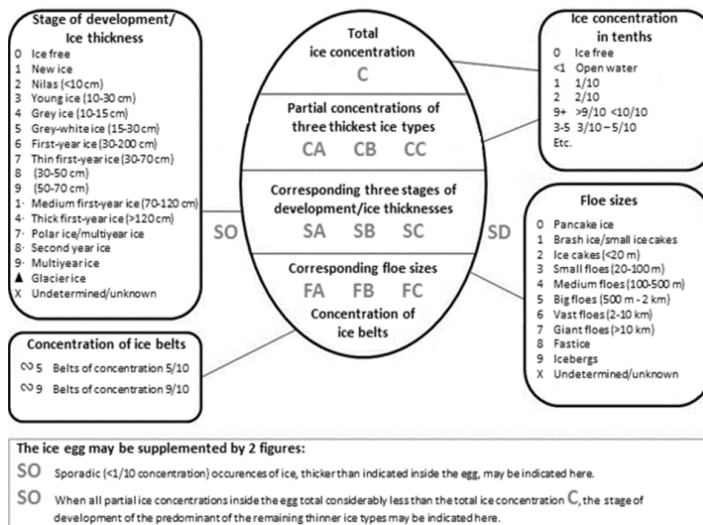


Fig. 1. The international code used to describe sea-ice on sea-ice charts according to its stage of development, ice concentration and ice floe sizes (<https://www.dmi.dk/en/hav/groenland-og-arktisk-iskort/1258/>).

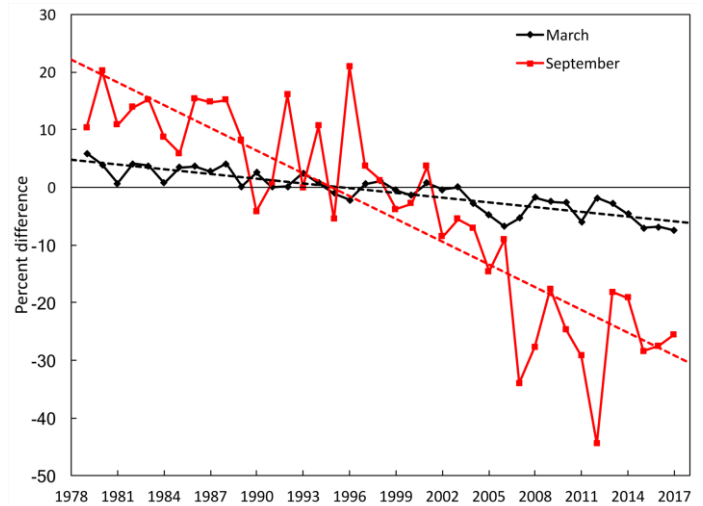


Fig. 2. Time-series of Northern Hemisphere ice extent anomalies in March (the month of maximum ice extent) and September (the month of minimum ice extent). The anomaly value for each year is the difference (in %) in ice extent relative to the mean values for the period 1981-2010. The black and red dashed lines are least squares linear regression lines. The slopes of these lines indicate ice losses of -2.7% and -13.2% per decade in March and September, respectively. Both trends are significant at the 99% confidence level (from Perovich et al., 2017)

Sea-ice strength parameters (tensile, flexural, shear, compressive, multi-axial and borehole) are known to be low for the early stages of ice development up to thin first year-ice. These strength parameters increase considerably for medium and thick first-year ice and are much larger for old ice. For example, the typical range of compressive ice strength values are 0.5 to 5.0 MPa for first-year ice and can be much higher for old ice with values of up to 15 MPa (Timco and Weeks, 2010).

### Arctic Sea-Ice Extent by Regions: Varying Long-Term Trends

Sea-ice extent of the northern hemisphere has been trending downwards over the past 40 years (Fig. 2) with the largest trends occurring in late summer and with smaller, but still statistically significant downward trends in late winter. In late summer, the ten lowest sea-ice extents have occurred in the last 11 years (Parkinson and DiGirolamo, 2016). In late winter, the most recent three years represent the lowest recorded sea-ice extent since satellite measurements of polar sea ice extent have been recorded.

Based on analysis of the satellite-based ice extent data from 1979-2006, the downward trend has large variations among different regions of the northern hemisphere with the largest annual reductions occurring on the continental margin of Russia and in the Arctic Ocean including the Canada Basin, Beaufort Sea and Chukchi Sea. Intermediate level reductions have occurred in the Greenland Sea and Baffin Bay and smaller with still statistically significant reductions in Hudson Bay and the Seas of Okhotsk and Japan. In other subareas, the reductions were smaller and not statistically significant (Parkinson and Cavalieri, 2008).

The age of sea-ice is another key descriptor of the state of the sea-ice cover. Derived from satellite observations and drifting buoy records, ice age is an indicator for ice physical properties, including thickness and ice strength (Tschudi et al., 2016). Over the past 40 years, the ice

age has greatly decreased in the northern hemisphere (Fig. 3) with old ice categories decreasing from over 40% of total ice extent to just over 20%. An even greater relative decrease has occurred in ice age categories of more than four years age to extremely low levels in the past decade. Since 2007, the reduction of old ice has been very large in the Beaufort Sea and Canada Basin (Maslanik et al., 2011).

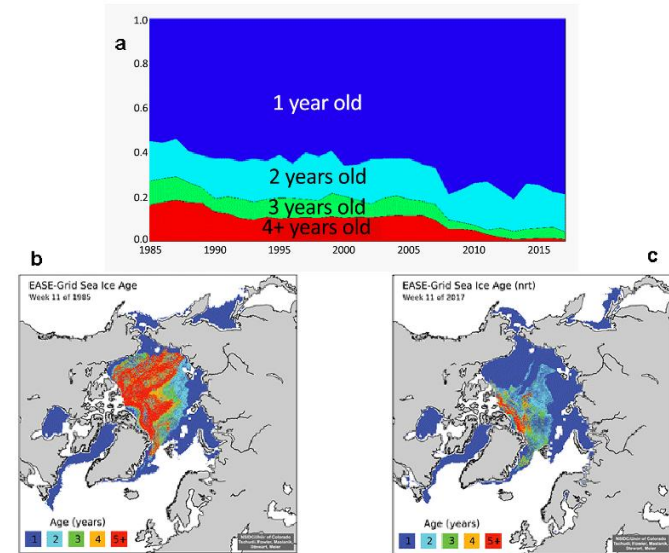


Fig. 3. (a) Sea ice age coverage by year, 1985–2017. Sea ice age coverage maps for (b) March 1985 and (c) March 2017 (adapted from Perovich et al., 2017).

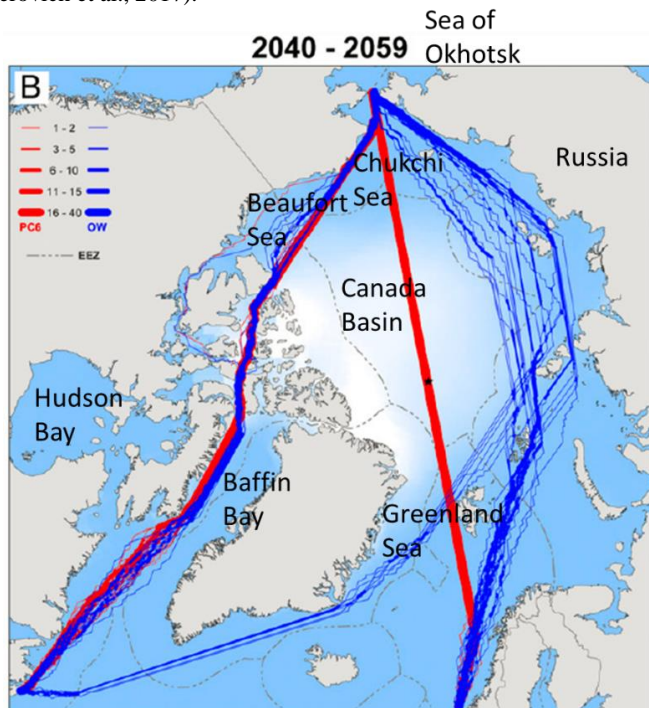


Fig. 4. Computed September navigation routes for hypothetical ships seeking to cross the Arctic Ocean between the North Atlantic (Rotterdam, The Netherlands and St. John's, Newfoundland) and the Pacific (Bering Strait) during consecutive years 2040–2059 scenario as driven by ensemble-average climate model projections of sea-ice concentration and thickness (Smith and Stephenson, 2013). The red and blue tracks designate ships that have ice class designs or open water commercial designs, respectively.

The effect of the reduced sea-ice extent is already resulting in increased activities such as shipping, tourism, and resource extraction. Traffic and cargo volume using the Northern Sea Route (NSR) ports has increased over recent past years (Fig. 4, Smith and Stephenson, 2013).

As sea ice extent and age/thickness continue to decrease, ship passages directly across the Arctic Ocean in international waters via the Trans-Arctic shipping route may become a reality by mid-century (Smith and Stephenson, 2013) and even sooner for ice-breaking cargo ships.

## ICE THICKNESS AND DEFORMATION PROCESSES

### Geometry of Sea Ice

As the ocean surface freezes, heat is transferred from the ocean to the atmosphere. Once an ice cover is established, the ocean heat must conduct through the ice before reaching the atmosphere. As the ice thickens, the rate of heat conduction is reduced, ultimately reaching a thermodynamic equilibrium thickness where the insulation of the ice canopy balances the conductive heat transfer. The sea-ice has then reached its maximum thickness attainable through thermodynamic growth, which is up to 3 m in the Arctic (Wadhams, 2000).

The thickness of sea-ice further increases through mechanical deformation to attain thicknesses much greater than the thermodynamic equilibrium limit (Fig. 5). The complex dynamical response of sea-ice to environmental forcing causes collisions between ice floes. When two ice sheets or an ice sheet and the seabed collide, to the point of ice failure, the sea-ice responds by buckling, rafting, ridging, and fracturing (Eicken, 2018). Buckling occurs most commonly in thin ice; in thicker ice the tensile stresses lead to fracture. Rafting is the slippage of one ice sheet over the surface of another. Very thick features are generated through ridging – the thinner colliding ice floe fractures into blocks which are then piled above and below the sheet. These blocks refreeze into a consolidated ice feature with a much higher draft than the source ice sheet. Observations of very deep features in the Beaufort Sea suggest that their maximum draft is constrained. The ice draft  $h$  of level ice can generate features of  $20 \cdot h^{1/2}$  maximum draft (Amundrud et al., 2004). An Arctic maximum level ice draft of about 3 m is consistent with a maximum ice draft of 35 m for deformed features.

The failure modes described above create a sea-ice cover inundated with fractures. Flaws in sea-ice can also occur due to thermal fluctuations (Lewis, 1998) and flexing stresses due to surface waves passing through the ice medium (Asplin et al., 2012). The fractured sea-ice cover is a collection of ice floes and the atmospheric and ocean current stresses lead to differential motion of these floes (see Ice Velocity Physical Processes below). The resulting openings between floes, called leads, range in width over scales of meters to kilometers (Fig. 5 and Fig. 13, for example). New thin ice is formed within these leads which then easily deforms under narrowing of the adjoining relatively thicker ice cover.

Hummocky ice is another important geometric feature of sea-ice. When sustained forcing converges ice floes, continuous compressive events within first-year sea-ice lead to a field of ragged morphology. The floes are rotated and forced out of the plane of undeformed sea-ice to create massive features with mean draft of about 4 m and horizontal widths of several hundreds of meters (Fissel et al., 2013).

The ice features described above occur with varying frequency. Fissel et al. (2015) define a massive ice feature (MIF) as those with a cross-sectional area exceeding 200 m<sup>2</sup> and an ice draft profile exceeding 2 m. Based on year-long time-series of ice draft acquired between 2009 and



2011, MIF events accounted for 1-2% of the total ice transiting the outer and inner continental slope of the Canadian Beaufort Sea. In the highly dynamic ice regime of Fram Strait over 2008-2009 and 2012-2013, the number of MIF events was 5.5 times greater than in the Canadian Beaufort Sea and accounted for 9-13% of the total observed ice (Fissel et al., 2015).

### Measurement Methods

To monitor adequately the range of ice actions in an area of interest, long-term, continuous, and high-resolution measurements of ice thickness are required (International Organization for Standardization (ISO), 2010). Over an entire season in highly mobile locations, thousands of kilometers of ice can transit by and be peppered with episodes of open water, thickening level ice, deep ice keels, and rubble fields. Often, multi-year monitoring programs are necessary to elucidate the seasonal patterns in the ice cover evolution and to observe the large inter-annual variability in some ice regimes. Significant ice actions can result from ice features with widths as small as 30 to 50 m.

Moored upward-looking sonars (ULS) have been in use in offshore industrial and research studies since the 1990s (Melling et al., 1995; Fissel et al., 2013; Fig. 6) and are a reliable method for observing sea-ice thickness. Ice profiling sonar (IPS) provides the long-term (1+ years), continuous and frequent (1 Hz), high-resolution (5-10 cm), and localized measurements of sea-ice thickness required to characterize physical environmental properties critical to engineering for offshore polar structures (ISO, 2010) including ice thickness, ice presence, ice morphology, and ice type. Research is ongoing for the use of the IPS-based high-resolution morphology measurements and the acoustic signature of ice targets to distinguish multi-year from first-year ice.

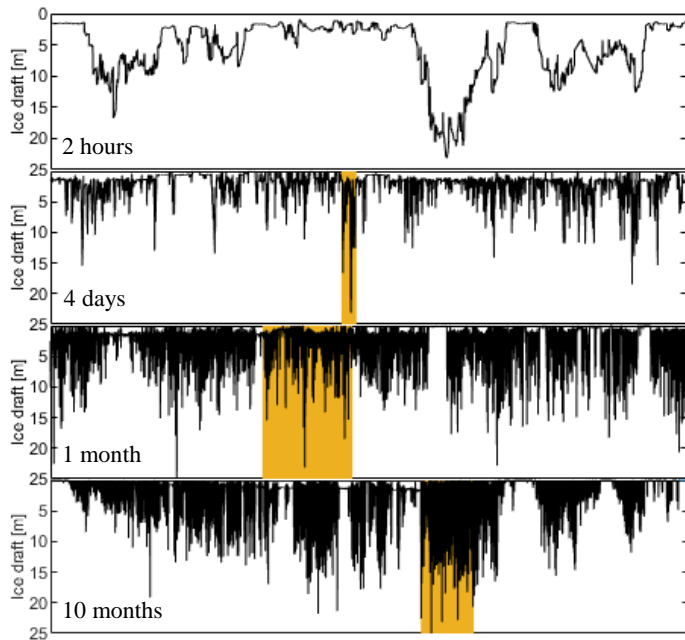


Fig. 5. Upward-looking sonar sea ice draft profiles spanning (from top to bottom) two hours, four days, one month, and ten months at a site on the continental margin of the Canadian Beaufort Sea. Each coloured area shows the segment spanned by the plot above it. The growth in the level undeformed ice and the thick features constructed from this material are evident. The bottom panel shows the full ice season from freeze-up to break-up, spanning 3000 km, and containing 5500 unique features exceeding 5 m thickness.

The subsurface ULS sits either in a frame directly on the seabed or in a taut-line configuration (Fig. 7) suspended within the water column. Most of these mooring assemblies are deployed and recovered from the surface without the need for divers or underwater vehicles.

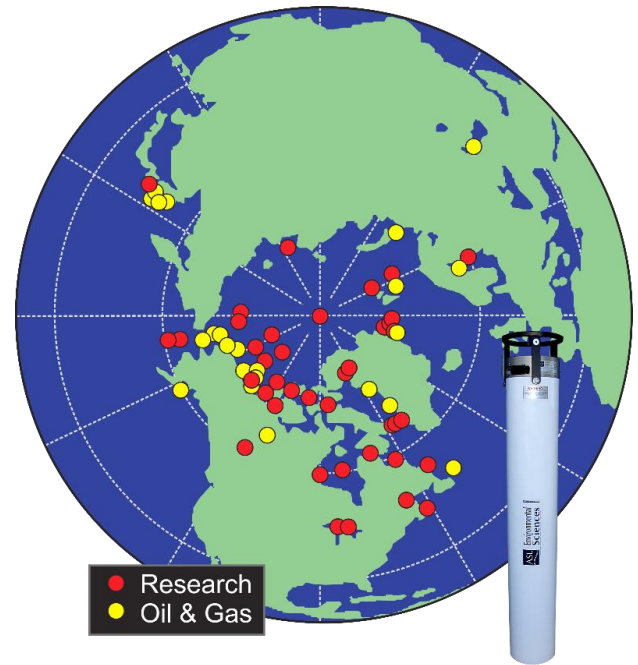


Fig. 6. Some of the locations of deployed ice profiling sonar (IPS) upward-looking sonar (ULS) instrumentats since the 1990s in the Northern Hemisphere.

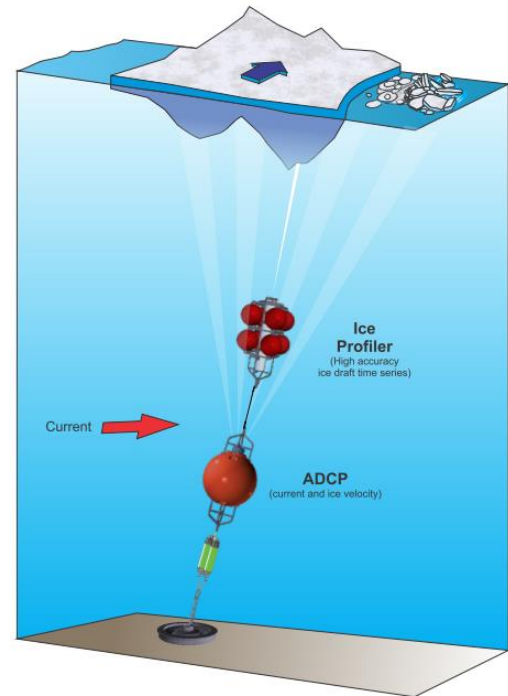


Fig. 7. A taut-line mooring assembly using upward-looking sonar (ULS) to observe the sea ice thickness with an Ice Profiling Sonar (IPS). An Acoustic Doppler Current Profiler (ADCP) is incorporated on the same or nearby mooring for coincident ice velocity and ocean current measurements. The mooring line can be instrumented with other sensors for measuring physical, biological and chemical properties. ([http://aslenv.com/Doc/IPS\\_taut\\_line\\_mooring.pdf](http://aslenv.com/Doc/IPS_taut_line_mooring.pdf)).

Space-based observations provide the broadest spatial coverage in the remote observation of sea-ice. This coverage along with the revisit time of consecutive observations (typically a few days), makes satellite imagery suitable for large study areas (e.g. shipping routes) and for characterizing the seasonal patterns in ice presence.

The operational CryoSat-2 mission and the upcoming IceSat-2 mission are purpose-built for ice thickness estimation. Many other spaceborne payloads have increased the availability and accessibility of earth observation datasets of ice presence and surface morphology including RADARSAT-2, Sentinels 1 and 3, SMOS, and TerraSAR-X, for example. Although an important tool in ice monitoring, space-based observations are limited by their low temporal and spatial resolutions and the data quality can vary depending on the environmental conditions.

Other methods for measuring ice thickness are noteworthy. For certain industrial applications and operations, an ice thickness survey along a route or across a gridded area is sufficient. In these cases, instrumentation can be used above the sea-ice surface from handheld devices, towed sleds, and airborne platforms. The sled-based and airborne sensor include electromagnetic (EM) systems which induce small currents in the seawater at the ice-seawater interface and the resulting magnetic field is measured to determine the distance to this interface while a laser altimeter determines the distance to the surface; the difference leads to the snow-ice thickness (Haas et al., 2009). These instruments have been widely used in airborne and sled-based geotechnical surveys and environmental studies.

Few remote sensing methods can match the accuracy of spot measurements by manually coring a sea ice sample. Snow depth as well as ice thickness is readily measured by this method. The sampled snow and ice can also be tested for various physical and mechanical properties (Johnston and Timco, 2005). The limitations of this approach for long-term and dense sea ice monitoring are obvious; however, manual ice thickness observations will always remain vital to the calibration of remote sensing methods and for sampling of the physical properties of the ice and snow.

## ICE VELOCITY PHYSICAL PROCESSES

Our understandings of sea-ice velocity have advanced enormously over the past 35 years. This is due, in large part, to much improved methods for making detailed and large-scale measurements of the sea-ice velocity field of the Arctic Ocean and adjoining areas. These measurements have provided previously unavailable sources of information on the deformation and fracturing of sea-ice across a wide range of spatial (1–1000 km) and temporal (1 h–30 years) scales (Weiss, 2013).

### Measurement Methods

While observations from ships navigating regions of moderate ice concentrations and the tracks of ships beset in ice are available since the late 1800s (Colony and Thorndike, 1984), these measurements were very sparse in terms of temporal resolution (sub-daily), accuracy (~ 1 km) and with very limited spatial coverage. With advancements in sensor technology and in polar orbiting satellite access to remote polar regions, the techniques for measuring sea ice drift have evolved dramatically starting in the 1970s. Beginning in 1979, the Arctic Ocean Buoy Program performed widespread measurements of sea-ice motion using drifting buoys mounted on ice floes which obtained positions and communicated via polar orbiting satellites, i.e. drifters (iabp.apl.washington.edu, 2018). Measurements of ice floe position

were obtained several times each day, with an accuracy of 0.1–0.3 km and much improved spatial coverage (Weiss, 2013).

This program was succeeded in 1991 by the still-operational International Arctic Buoy Program (IABP). An example of the detailed trajectories derived from these arrays of satellite-tracked buoys are shown in Fig. 8.

In the latter part of the 20<sup>th</sup> century, measuring ice drift via satellite imagery became possible through the use of sequential remote-sensing imagery by identifying ice floes which are used to determine the relative position of features within sequential images (Leppäranta, 2011). Algorithms have been developed for data from synthetic aperture radar (SAR) satellites for cross-correlation or feature tracking (Kwok et al., 1990). More recently, algorithms have been developed to extract sea ice motion from satellite passive microwave data using the cross-correlation method (Agnew et al., 1997; Kwok et al., 1998). The use of sequential all-weather satellite-imagery allows the derivation of daily, spatially extensive Lagrangian velocity maps of sea-ice velocities with spatial resolutions of many tens of kilometers (Fig. 9). This sequential satellite imagery ice velocity data is complementary to the higher temporal resolution but lower spatial resolution and coverage of the drifter data sets.

During the late 1980s, the use of upward-looking sonar (ULS) from moorings tethered to the ocean floor (Fig. 7) became a reliable source of sea ice draft and drift measurement (Belliveau, et. al., 1990; Melling, et. al., 1995; Fissel, et. al., 2013). The standard technology for this is the acoustic Doppler current profiler (ADCP) which measures the Doppler frequency shift of a backscattered acoustic pulse. When deployed with “bottom-track” mode, the ADCP employs its’ four sonar beams, angled at 20° from zenith, to determine the three-dimensional velocity of the ocean currents as well as the overhead ice pack.

ADCPs can be readily configured to obtain high-resolution (on a scale of minutes) ice velocity measurements continuously for deployments of one year or longer. Each ice velocity measurement is an average of an ensemble of pings which reduces the overall standard error in the ice velocity component speeds. This ice velocity measurement technology is complementary to the satellite drifter and sequential satellite imagery methods by providing much higher temporal resolution but more limited spatial coverage.

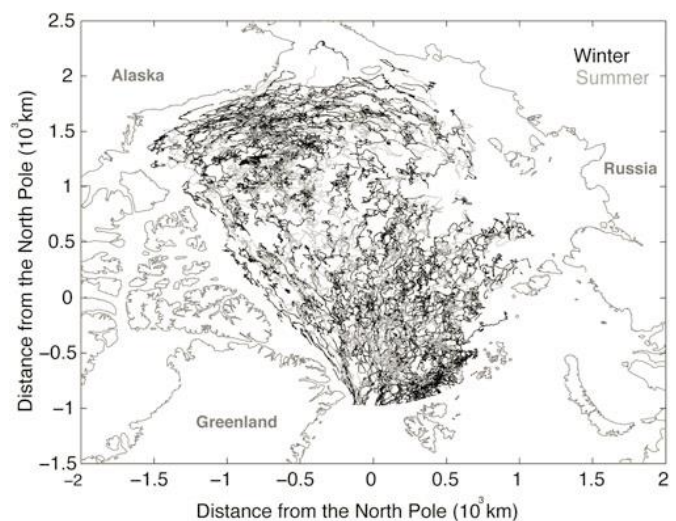


Fig. 8. IABP buoys trajectories recorded between December 1978 and December 2001 in the Arctic basin. The tortuous character of sea ice motion is obvious (adapted from Rampal et al., 2009).

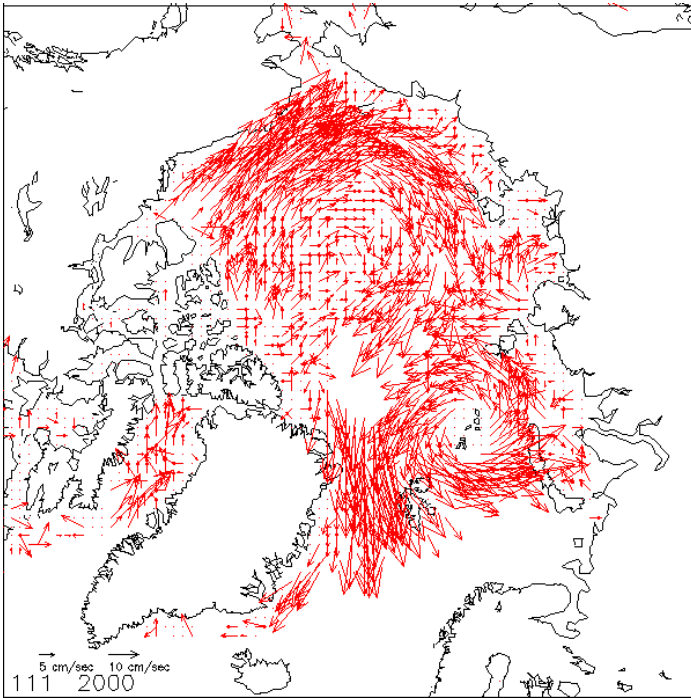


Fig. 9. Ice motion derived from sequential SSM/I passive microwave satellite images on 20 April 2000. (obtained from NSICS web site “Ice Motion from Passive Microwave: SMMR, SSM/I, SSMIS, and AMSR-E” at <https://nsidc.org/data/pm/nsidc0116-icemotion-smmr-ssmi>)

### Ice Velocity Processes and Distributions

The availability of drifter and sequential satellite imagery data sets have led to greatly improved understandings of sea-ice velocity. With the advent of drifter data sets in the late 1970s, pioneering studies were carried out of the sea-ice drift in response to wind forcing (Thorndike and Colony, 1982) and the decomposition of ice drift into a mean field driven by wind forcing and ocean circulation (Fig. 10) and the fluctuating field in form of random walk (statistical) field associated with atmospheric and oceanic turbulence (Colony and Thorndike, 1984).

The sea-ice velocity data sets can also be used to examine sea-ice deformation on various time and spatial scales by analysis of the dispersion field of sea-ice motion. Large differences in the statistical properties of dispersion are found between sea-ice and turbulent fluids, in particular the presence of strong space/time coupling of sea-ice deformation towards small spatial (and temporal) scales (Weiss, 2013). This type of deformation has no equivalence in turbulent fluids like the atmosphere and ocean, but it is similar to the deformation characteristics of the upper Earth’s crust (Weiss, 2013). This result suggests that sea-ice has a strongly non-linear, brittle rheology which has been studied extensively from patterns of sea-ice fractures realized in satellite imagery and in laboratory studies (Schulson and Duval, 2009).

Based on these concepts, a simple statistical model is able to reproduce the scaling properties of sea-ice deformation in space and time as derived from observations (Weiss, 2013).

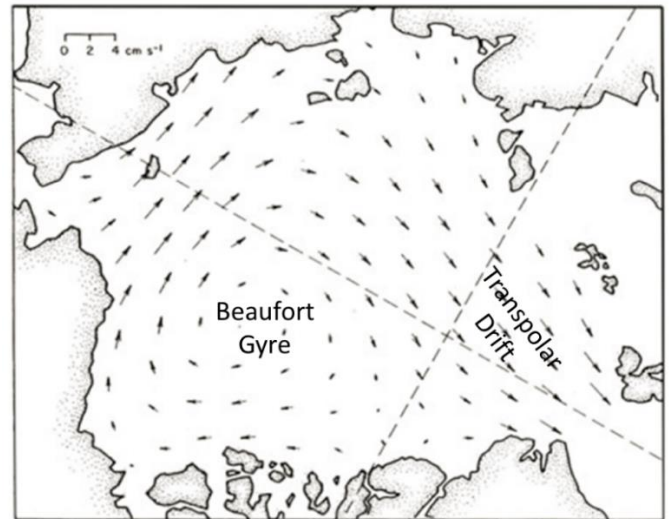


Fig. 10. A map of the mean field of Arctic sea-ice motion derived by Colony and Thorndike (1984) which depicts the Arctic General Circulation including the Beaufort Gyre and the Transpolar Drift Stream.

The analysis of sea-ice drift, deformation and fracturing provide important insights into the role of future Arctic sea-ice cover. The future sea-ice cover is simulated using climate models which couple the atmosphere, cryosphere (sea-ice) and ocean. These climate models have underestimated the observed sea-ice decline in recent years (Stroeve et al., 2012). The underestimates of sea-ice reduction by the models suggest that ice-free conditions in late summer which are presently predicted in the Arctic Ocean by the year 2100 may occur sooner with a possibility that ice-free summers may arrive within a few decades from now (Weiss, 2013). In addition, the present coupled climate models do not fully simulate the recent acceleration of ice motion (Rampal et al., 2011).

The export and loss of sea ice in the Arctic can be related to an increase of ice transport by the Transpolar Drift (Fig. 10). The Transpolar Drift is known to be related to the large scale atmospheric pressure patterns of the Arctic Oscillation (AO; also the Arctic Dipole Anomaly), in which years of a positive AO lead to a stronger Transpolar Drift and a reduced size of the Beaufort Gyre (Wang et al., 2009; Perovich and Richter-Menge, 2009). The positive phase of the AO has been shown to account for the reduction in late summer Arctic ice extent in some years of the early 1990s and in 2007 (Fig. 3).

Rampal et al. (2011) demonstrate that deficiencies in the existing climate model may result in an underestimate of the export of sea-ice by the Transpolar Drift. Possible reasons for the discrepancy between model and observed results include the use of a viscous-plastic rheology, as is widely used in the sea-ice models for the coupled climate models. The viscous-plastic rheology conflicts with the non-linear brittle rheology discussed above; the latter rheology is consistent with the analysis of deformation and fracturing of sea-ice. Clearly more research on the processes of sea-ice drift, deformation and fracturing is required to adequately model the future rate of decline of sea-ice cover in the Arctic Ocean and adjoining seas (Weiss, 2013).



## CASE STUDY: VARIABILITY OF ICE VELOCITIES OVER DIFFERENT SPATIAL SCALES IN THE BEAUFORT SEA

### 2009-2011 Canadian Beaufort Sea Dense Array Measurement Program

A dense array (Fig. 11) of 9-10 upward looking sonar (ULS) instruments operating from subsurface moorings in the Canadian Beaufort Sea were used to provide accurate (0.4%), continuous and spatially detailed measurements of ice velocity over two full years: 2009-2011 using ADCP instruments (Fig. 6). The moorings were placed in water between 55 and 1010 m depth on the shelf and continental slope of the Canadian Beaufort Sea thereby spanning several topographic regimes between the middle slope and the middle shelf. The separation of moorings ranged between 4 and more than 100 km.

The analysis of the sea-ice velocity measurements (Ross et al., 2017) demonstrated the extent of spatial variability in ice drift across an approximately 100 km × 100 km region of the continental margin of the Canadian Beaufort Sea. At temporal scales of five days and longer, the sea-ice drift across the array is often consistent; however, this pattern is periodically interrupted by two significant effects. Firstly, when forcing results in convergent motion (towards the shore or the landfast ice edge), this leads to high ice concentration with further forcing resulting in increased internal ice stress. Secondly, when the wind forcing shifts to be directed away from shore resulting in divergent motion, there is a relatively rapid acceleration of the sea-ice drift.



Fig. 11. (top) The area in the Canadian Beaufort Sea where ice profiling sonars (IPS) have been deployed since the 1990s. (bottom) The locations of the dense array of moored instruments operated in the continental margin of the Canadian Beaufort Sea from 2009-2011 (Ross et al., 2017).

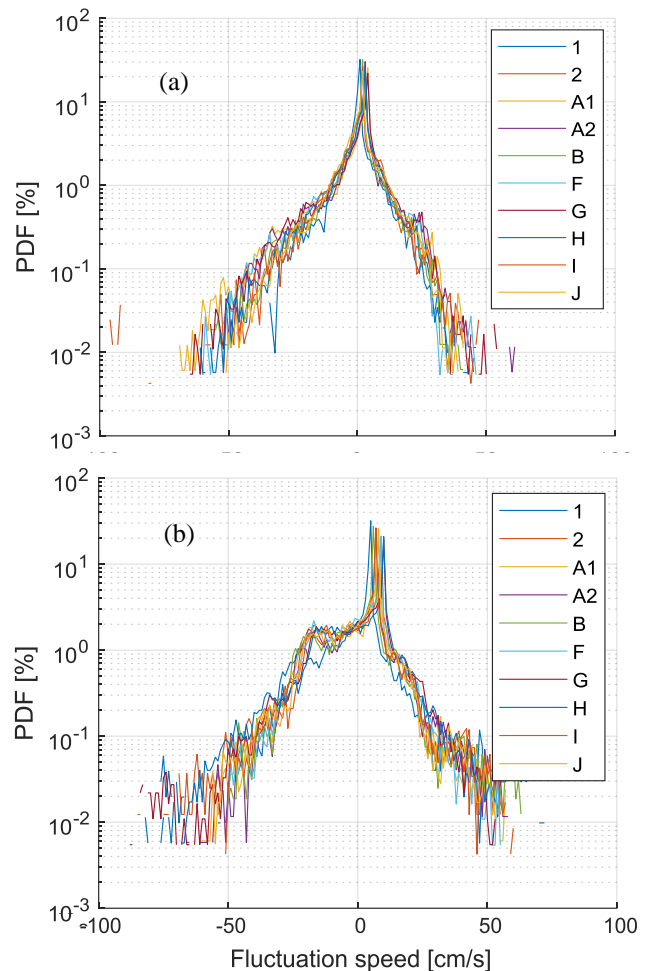


Fig. 12. Probability distribution function of fluctuation speeds in the (a) north/south and (b) east/west direction during 2009-2010 (Ross et al., 2017). Note that the velocities referred to here are the direction *towards* which the ice is moving. Fluctuation speeds are determined by subtracting the mean velocity field from the ice velocity time-series.

### Probability Distribution of Fluctuation Speeds

Ross et al. (2017) analyzed the probability distribution functions of the fluctuation speeds for each component (east/west, north/south) and each measurement year. The north/south results (Fig. 12a) present an approximate symmetric distribution of fluctuation speeds suggesting a lack of directionality bias in the forcing along this dimension. The east/west results (Fig. 12b) are very different and show a clear bias to westward fluctuation speeds particularly in the 0 to 20 cm/s range. As the fluctuation speeds are determined after removing the mean velocity field, the bias to westward fluctuations is unexpected. The mean velocity field itself is dominantly westward due to the prevalence of easterly winds and the influence of the Beaufort Gyre. The observed bias was attributed to the higher speeds that can be more readily reached under these conditions where fractures and consequently leads in the ice cover allow for westward acceleration; however, this result could also suggest shortcomings in the determination of the mean velocity field. This is the subject of ongoing research.

These broad observations appear to support the conclusions of Rampal et al (2009) that “sea ice dynamics is significantly influenced by the interplay of multiple fractures that are activated intermittently within the ice pack.”

## Small Scale Spatial Variability of Ice Velocities for Episodic Wind Forcing

Fig. 13 shows an example of the ice cover response to episodic wind forcing that leads to the observed small-scale spatial variability in ice drift across the measurement array. Between February 28, 2010 and March 11, 2010, easterly winds result in a dramatic fracturing event in the Canadian Beaufort Sea. The ice cover over the mooring array prior to this event was immobile and reaches speeds up to 30 cm/s within a few hours on March 6. Over the following five days, as the wind shifts direction, the ice cover experiences four oscillations between appreciable speeds and immobility. During each oscillation, the ice cover travels between about 2 and 25 km depending on the location within the array. These wind-driven ice velocity episodes can result in significant differential motion across the region. The interaction between ice floes, in the form of fracturing of the sea-ice cover, is suspected to be the main driver of this spatial variability. Given the highly deformed and fractured nature of the floating sea-ice cover, very different responses to nearly identical wind forcing of sea-ice floes can occur over distances as small as a few kilometers.

The ice drift response to external forcing varies seasonally as both the local and regional ice concentration evolves. However, even during the highest ice concentration episodes, the response can vary significantly under convergent and divergent forcing conditions. As a result, ongoing work aims to further segment the forcing into these two categories using the results of the MSC Beaufort Wind and Wave Reanalysis (Swail et al., 2007) which provides hourly modeled wind and wave parameters at 5 km grid resolution. Between October 2009 and October 2011, we found wind forcing events sustained in directions for 24 hours or longer that should lead to convergent (69 events) and divergent (80 events) ice drift response. This set of over 150 events at a fine spatial and temporal resolution is a unique database for further examining the complex ice drift response to relatively consistent forcing.

## CONCLUSIONS AND DISCUSSION

We have summarized the progress realized from sea-ice research over the past 30 to 40 years due in large part to improved measurements arising from earth observing satellites and year-long continuous measurements of the underside of sea ice from below using subsurface instrumented moorings.

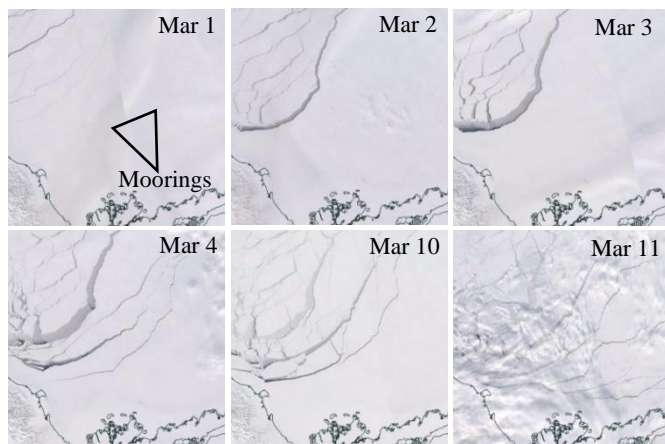


Fig. 13. Aqua MODIS images of a fracturing event in 2010 in the Canadian Beaufort Sea between March 1 and 11. (<https://worldview.earthdata.nasa.gov>).

The geometry of sea-ice is highly variable and complex. The response of sea ice to wind and other types of forcing has been shown to be highly complex even on a small spatial scale of tens of kilometers. The underlying causes of this complexity can be attributed, in part, to the deformation and fracturing processes of sea ice, which are not fully understood.

The sea-ice cover of the Arctic has changed considerably over the past 30 years towards much reduced coverage especially in the summer and early fall. As a result, greater access to the Arctic for commercial shipping and for offshore oil and gas exploration is envisioned in the remainder of this century. However, the rate of further reductions in ice extent remain uncertain which will require further advances in our understanding of sea-ice processes.

## ACKNOWLEDGEMENTS

The authors wish to acknowledge the ArcticNet/Industry Partnership Program for funding the 2009-2011 Beaufort Sea measurement program and Dr. Humfrey Melling of the Department of Fisheries and Oceans, Institute of Ocean Sciences, who provided some of the data sets used in the case study results presented.

## REFERENCES

- Agnew, T., Le, H. and Hirose, T. (1997). "Estimation of large-scale sea-ice motion from SSM/I 85.5 GHz imagery", *Annals of Glaciology*, 25, p. 305-311. doi: 10.3189/S0260305500014191
- Amundrud, T., Melling, H. and Ingram, R. (2004). "Geometrical constraints on the evolution of ridged sea ice", *Journal of Geophysical Research*, 109(C6). doi: 10.1029/2003JC002251
- Asplin, M., Galley, R., Barber, D. and Prinsenberg, S. (2012). "Fracture of summer perennial sea ice by ocean swell as a result of Arctic storms", *Journal of Geophysical Research: Oceans*, 117(C6). doi: 10.1029/2011JC007221
- Belliveau, D., Bugden, G., Eid, B. and Calnan, C. (1990). "Sea Ice Velocity Measurements by Upward-Looking Doppler Current Profilers", *Journal of Atmospheric and Oceanic Technology*, 7(4), p. 596-602. doi: 10.1175/1520-0426(1990)007<0596:SIVMBU>2.0.CO;2
- Colony, R. and Thorndike, A. (1984). "An estimate of the mean field of Arctic sea ice motion", *Journal of Geophysical Research*, 89(C6), p. 10623-10629. doi: 10.1029/JC089iC06p10623
- Dansereau, V., Weiss, J., Saramito, P. and Lattes, P. (2016). "A Maxwell elasto-brittle rheology for sea ice modelling", *The Cryosphere*, 10(3), p. 1339-1359. doi: 10.5194/tc-10-1339-2016
- Eicken, H. (2018). *Sea ice deformation features and processes*. Available at: [http://www2.gi.alaska.edu/~eicken/he\\_teach/GEOS615icenom/deform/seaicedef.htm](http://www2.gi.alaska.edu/~eicken/he_teach/GEOS615icenom/deform/seaicedef.htm)
- Feltham, D., Untersteiner, N., Wettlaufer, J. and Worster, M. (2006). "Sea ice is a mushy layer", *Geophysical Research Letters*, 33(14). doi: 10.1029/2006GL026290
- Fissel, D., Chave, R., Clarke, M., Johnston, P., Borg, K., Marko, J., Ross, E., Buermans, J. and Stone, M. (2013). "Advances in Moored Upward Looking Sonar Systems for Long Term Measurement of Arctic Ice and Oceanography", in: *OCEANS 2013 MTS/IEEE San Diego*. San Diego, CA, USAIEEE. Available at: <http://dx.doi.org/10.23919/OCEANS.2013.6741279>
- Fissel, D., Ross, E., Sadowy, D. and Wyatt, G. (2015). "The Distribution of Massive Ice Features by Ice Types from Multi-Year Upward Looking Sonar Ice Draft Measurements", in: *OTC Arctic Technology Conference*. Copenhagen, Denmark, Offshore Technology Conference. Available at: <http://dx.doi.org/10.4043/25557-ms>



- Girard, L., Bouillon, S., Weiss, J., Amitrano, D., Fichet, T. and Legat, V. (2011). "A new modeling framework for sea-ice mechanics based on elasto-brittle rheology", *Annals of Glaciology*, 52(57), p. 123-132. doi: 10.3189/172756411795931499
- Gow, A. and Tucker, W. (1991). *Physical and Dynamic Properties of Sea Ice in the Polar Oceans*. U.S. Army Corps of Engineers, Cold Regions Research & Engineering Laboratory, p. 63. Available at: <http://www.dtic.mil/dtic/tr/fulltext/u2/a256303.pdf>
- Haas, C., Lobach, J., Hendricks, S., Rabenstein, L. and Pfaffling, A. (2009). "Helicopter-borne measurements of sea ice thickness, using a small and lightweight, digital EM system", *Journal of Applied Geophysics*, 67(3), p. 234-241. doi: 10.1016/j.jappgeo.2008.05.005
- Hamilton, J. (2011). "The Challenges of Deep Water Arctic Development", in: *Twenty-first International Offshore and Polar Engineering Conference*. Maui, Hawaii, USA, International Society of Offshore and Polar Engineers (ISOPE). Available at: <https://www.onepetro.org/conference-paper/ISOPE-11-137>
- iaabp.apl.washington.edu. (2018). *International Arctic Buoy Programme*. [online] Available at: <http://iaabp.apl.washington.edu/>
- ISO (International Organization for Standardization) (2010). *Petroleum and natural gas industries - Arctic offshore structures*. (Standard ISO/FDIS 19906:2010(E)). Retrieved from: [www.iso.org/standard/33690.html](http://www.iso.org/standard/33690.html)
- Johnston, M. and Timco, G. (2005). *Validating the strength algorithm for sub-arctic ice with field measurements from Labrador*. National Research Council Canada, Canadian Hydraulics Centre. Available at: <http://dx.doi.org/10.4224/12327506>
- Kwok, R., Curlander, J., McConnell, R. and Pang, S. (1990). "An ice-motion tracking system at the Alaska SAR facility", *IEEE Journal of Oceanic Engineering*, 15(1), p. 44-54. doi: EC Accession Number: 3629804 DOI: 10.1109/48.46835
- Kwok, R., Schweiger, A., Rothrock, D., Pang, S. and Kottmeier, C. (1998). "Sea ice motion from satellite passive microwave imagery assessed with ERS SAR and buoy motions", *Journal of Geophysical Research: Oceans*, 103(C4), p. 8191-8214. doi: 10.1029/97JC03334
- Lepparanta, M. (2011). *The Drift of Sea Ice*. 2nd ed. Berlin, Heidelberg Springer.
- Lewis, J. (1998). "Thermomechanics of pack ice", *Journal of Geophysical Research: Oceans*, 103(C10), p. 21869-21882. doi: 10.1029/98JC01256
- Maslanik, J., Stroeve, J., Fowler, C. and Emery, W. (2011). "Distribution and trends in Arctic sea ice age through spring 2011", *Geophysical Research Letters*, 38(13). doi: 10.1029/2011GL047735
- Meier, W., Hovelsrud, G., Van Oort, B., Key, J., Kovacs, K., Michel, C., Haas, C., Granskog, M., Gerland, S., Perovich, D., Makshtas, A. and Reist, J. (2014). "Arctic sea ice in transformation: A review of recent observed changes and impacts on biology and human activity", *Reviews of Geophysics*, 52(3), p. 185-217. doi: 10.1002/2013RG000431
- Melling, H., Johnston, P. and Riedel, D. (1995). "Measurements of the Underside Topography of Sea Ice by Moored Subsea Sonar", *Journal of Atmospheric and Oceanic Technology*, 12(3), p. 589-602. doi: 10.1175/1520-0426(1995)012<0589:MOTUTO>2.0.CO;2
- NSIDC (National Snow and Ice Data Center), 2018. *All about sea ice*. Available at: <https://nsidc.org/cryosphere/seaiice/index.html>.
- Parkinson, C. and Cavalieri, D. (2008). "Arctic sea ice variability and trends, 1979-2006", *Journal of Geophysical Research*, 113(C7). doi: 10.1029/2007JC004558
- Parkinson, C. and DiGirolamo, N. (2016). "New visualizations highlight new information on the contrasting Arctic and Antarctic sea-ice trends since the late 1970s", *Remote Sensing of Environment*, 183, p. 198-204. doi: 10.1016/j.rse.2016.05.020
- Perovich, D. and Richter Menge, J. (2009). "Loss of Sea Ice in the Arctic", *Annual Review of Marine Science*, 1(1), p. 417-441. doi: 10.1146/annurev.marine.010908.163805
- Perovich, D., Meier, W., Tschudi, M., Farrell, S., Hendricks, S., Gerland, S., Haas, C., Krumpen, T., Polashenski, C., Ricker, R. and Webster, M. (2017). *Arctic Report Card: Update for 2017 - Sea Ice*. Available at: <http://www.arctic.noaa.gov/Report-Card/Report-Card-2017/ArtMID/7798/ArticleID/699/Sea-Ice>
- Rampal, P., Weiss, J., Dubois, C. and Campin, J. (2011). "IPCC climate models do not capture Arctic sea ice drift acceleration: Consequences in terms of projected sea ice thinning and decline", *Journal of Geophysical Research*, 116. doi: 10.1029/2011JC007110
- Rampal, P., Weiss, J., Marsan, D. and Bourgoin, M. (2009). "Arctic sea ice velocity field: General circulation and turbulent-like fluctuations", *Journal of Geophysical Research: Oceans*, 114(C10). doi: 10.1029/2008JC005227
- Ross, E., Fissel, D. and Borg, K. (2017). "Spatial Variability of Sea Ice Velocity in the Continental Margin of the Canadian Beaufort Sea from a Dense Array of Moored Upward Looking Sonar Instruments", in: *Twenty-seventh International Ocean and Polar Engineering Conference*. San Francisco, CA, USA International Society of Offshore and Polar Engineers (ISOPE)
- Schulson, E. and Duval, P. (2009). *Creep and Fracture of Ice*. Cambridge University Press (CUP).
- Smith, L. and Stephenson, S. (2013). "New Trans-Arctic shipping routes navigable by midcentury", *Proceedings of the National Academy of Sciences*, 110(13), p. E1191-E1195. doi: 10.1073/pnas.1214212110
- Stroeve, J., Kattsov, V., Barrett, A., Serreze, M., Pavlova, T., Holland, M. and Meier, W. (2012). "Trends in Arctic sea ice extent from CMIP5, CMIP3 and observations", *Geophysical Research Letters*, 39(16). doi: 10.1029/2012GL052676
- Swail, V., Cardone, V., Callahan, B., Ferguson, M., Gummer, D. and Cox, A. (2007). "The MSC Beaufort Wind and Wave Reanalysis", in: *10th International Workshop on Wave Hindcasting and Forecasting and Coastal Hazard Symposium*. North Shore, Oahu, HI, USA
- Thorndike, A. and Colony, R. (1982). "Sea ice motion in response to geostrophic winds", *Journal of Geophysical Research*, 87(C8), p. 5845. doi: 10.1029/JC087iC08p05845
- Timco, G. and Weeks, W. (2010). "A review of the engineering properties of sea ice", *Cold Regions Science and Technology*, 60(2), p. 107-129. doi: 10.1016/j.coldregions.2009.10.003
- Tschudi, M., Stroeve, J. and Stewart, J. (2016). "Relating the Age of Arctic Sea Ice to its Thickness, as Measured during NASA's ICESat and IceBridge Campaigns", *Remote Sensing*, 8(12), p. 457. doi: 10.3390/rs8060457
- Wadhams, P. (2000). *Ice in the Ocean*. 1st ed. Amsterdam Gordon and Breach Science Publishers.
- Wang, J., Zhang, J., Watanabe, E., Ikeda, M., Mizobata, K., Walsh, J., Bai, X. and Wu, B. (2009). "Is the Dipole Anomaly a major driver to record lows in Arctic summer sea ice extent?", *Geophysical Research Letters*, 36(5). doi: 10.1029/2008GL036706
- Weiss, J. (2013). *Drift, Deformation, and Fracture of Sea Ice - A Perspective Across Scales*. 1 ed. Springer Netherlands.
- Weiss, J. (2017). "Exploring the 'solid turbulence' of sea ice dynamics down to unprecedented small scales", *Journal of Geophysical Research: Oceans*, 122(8), p. 2169-9291. doi: 10.1002/2017JC013236